Available online at www.sciencedirect.com

ScienceDirect

journal homepage: www.elsevier.com/locate/he

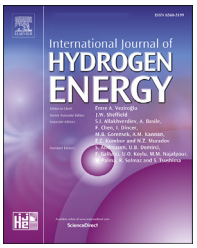

# Favourable band edge alignment and increased visible light absorption in $\beta$-$MoO_3$/$\alpha$-$MoO_3$ oxide heterojunction for enhanced photoelectrochemical performance

*Nisha Kodan* [a], *Aadesh P. Singh* [b], *Matthias Vandichel* [b], *Björn Wickman* [b], *B.R. Mehta* [a,*]

[a] *Department of Physics, Indian Institute of Technology, Hauz Khas, New Delhi 110016, India*
[b] *Division of Chemical Physics, Department of Physics, Chalmers University of Technology, SE-41296 Göteborg, Sweden*

ARTICLE INFO

*Article history:*
Received 22 January 2018
Received in revised form
20 June 2018
Accepted 23 June 2018
Available online xxx

*Keywords:*
Solar hydrogen
Photoelectrochemical (PEC) cell
Oxygen partial pressure
DFT Calulations
$MoO_3$-polymorphs
Oxygen evolution reaction (OER)

ABSTRACT

Optimum band gap values, favourable band edge positions and stability in the electrolyte are critical parameters required for a semiconductor to have efficient photoelectrode properties. The present investigation carried out on the phase pure $\alpha$ & $\beta$ $MoO_3$ thin film shows that the low bandgap $\beta$-$MoO_3$ possesses a mis-alignment with the water oxidation potential, while a more suitable band alignment is observed for the comparatively large bandgap $\alpha$-$MoO_3$. Both experimental and DFT calculations show that the valence edge of the orthorhombic ($\alpha$-$MoO_3$) phase is located at a higher energy (0.9 eV higher in VB-XPS and 1 eV higher in the DOS plots) than the monoclinic ($\beta$-$MoO_3$) phase, while the conduction edge value is roughly at the same energy level (−2.5 eV) in both polymorphs. Based on the above investigations, an all oxide heterojunction comprising of $\beta$-$MoO_3$/$\alpha$-$MoO_3$ is found to be suitable for improved PEC performance due to favourable energy band diagram and increased visible light absorption in $\beta$-$MoO_3$. Significantly higher cathodic photocurrent is observed for the $\beta$-$MoO_3$/$\alpha$-$MoO_3$ (1.6 mA/cm$^2$ at applied bias of $-0.3V_{RHE}$ under simulated 1 sun irradiation) as compared to the very low anodic response in $\beta$-$MoO_3$ (~1.0 nA/cm$^2$) and $\alpha$-$MoO_3$ (32 μA/cm$^2$).



## Introduction

Solar induced splitting of water in photoelectrochemical (PEC) cell appears to be the most promising, economically viable and sustainable way for the production of hydrogen. PEC cell integrates solar energy harvesting and water electrolysis into a single event on photoactive material surface. After the first report of Fujishima and Honda, significant research has been carried out during the last decades on transition metal oxides such as $TiO_2$, $WO_3$, ZnO and $Fe_2O_3$ for photocatalytic and photoelectrochemical water oxidation to produce chemical fuels such as hydrogen [1–4]. For an efficient photo-electrochemical water splitting, the required band gap of the

* *Corresponding author.*
E-mail address: brmehta@physics.iitd.ac.in (B.R. Mehta).
https://doi.org/10.1016/j.ijhydene.2018.06.138
0360-3199/

photoanode material should be optimum to absorb photons efficiently and band edge alignment favourable for photogenerated charge carriers ($e^-/h^+$) to be separated to prevent recombination. For an efficient photogenerated charge separation in PEC cell, the band edge positions of a semiconductor photoanode must be energetically and kinetically able to perform a desired water splitting reaction in such a way that photogenerated hole can be transported to the electrode surface to oxidize water and at the same time the photogenerated electron should move to the counter electrode surface to participate in the reduction reaction. In recent years, molybdenum trioxide ($MoO_3$) has received an increased attention as a possible photoanode material for PEC water splitting [5,6]. $MoO_3$ exhibits superior photo-physical and photo-chemical properties and also gained a special attention because of its multifaceted structural and functional properties [7,8]. $MoO_3$ is considered to be an n-type semiconductor with wide band gap (≥3 eV) [9,10] however, some studies have reported it to be a p-type semi-conductor [11]. $MoO_3$ can occur in different phases: orthorhombic (α-$MoO_3$; thermodynamically stable), monoclinic (β-$MoO_3$; metastable), high pressure monoclinic ($MoO_3$-II), and hexagonal (h-$MoO_3$) structures [12,13]. Out of these phases, the α-$MoO_3$ and β-$MoO_3$ are the most common polymorphs. Both α-$MoO_3$ and β-$MoO_3$ have been synthesized by various techniques in nanocrystalline, polycrystalline thin film and powder form and studied for their optical, electronic and chemical properties for electrochromic display devices [14,15], photocatalysis, solid-state micro-batteries [16,17], gas sensors [18] and bulk hetero-junction solar cells [19,20]. The bandgap of $MoO_3$ is observed to be in the range of 3.1–3.3 eV and 2.6–2.8 eV for the α-$MoO_3$ and β-$MoO_3$, respectively [21–23]. Photoactivity of different phases could be different as it depends upon the optical properties, electronic charge density, morphology and electronic band structure. As a result of differences in optical and electronic properties, it is likely to assume that the photoelectrochemical properties of the α-$MoO_3$ and β-$MoO_3$ should be markedly different. For photoelectrochemical water splitting applications, it is important to determine the structural and electronical properties of these polymorphs of $MoO_3$ and predict the band edge alignment to identify the mechanism of how photo-generated charge carriers transfer at the respective oxidation and reduction sites during the photoelectrochemical reaction. However, there are no reports available in the literature to date to compare the band alignment with respect to water redox potential, neither theoretically nor experimentally. Furthermore, there are no detailed reports on the positions of valence and conduction band edges, and the optical absorption behavior of the α-$MoO_3$ and β-$MoO_3$ phases, which is very important for determining their suitability for photoelectrochemical applications.

In this work, computational simulations and detailed experimental characterization has been carried out to study the properties of phase pure α & β $MoO_3$ thin films. Variable angle spectroscopic ellipsometry, Kelvin probe force microscopy and valence band X-ray photoemission spectroscopy measurements have been done to determine energy band diagram of both the phases which is compared with electronic structure calculations. Both simulated and experimental results show a favourable band edge alignment for α-$MoO_3$ which is consistent with enhanced photoelectrochemical properties of α-$MoO_3$ thin films in comparison to β-$MoO_3$ phase. It is conjectured that a favourable band diagram of β-$MoO_3$/α-$MoO_3$ interface and higher optical absorption properties of β-$MoO_3$ phase can be combined to fabricate an all oxide heterojunction with enhanced PEC performance.

## Experimental details

### *Computational methods*

Density Functional Theory (DFT) is applied with the gradient corrected (GGA) exchange-correlation functional to study the properties of $MoO_3$ phases [24]. In particular, the Vienna Ab Initio Simulation Package (VASP) is used [25,26]. The one-electron Kohn-Sham orbitals are expanded in a plane wave basis set with a kinetic energy cut-off of 600 eV for bulk structures and 450 eV for surface slabs. Projector augmented wave (PAW) potentials are employed to describe the interaction between the valence electrons and the core [27]. Reciprocal space integration over the Brillouin zone is approximated with finite sampling using Monkhorst-Pack grids [28,29]. For bulk systems, the k-point grids ($k_1$, $k_2$, $k_3$) is chosen, such that their product with the norms of the unit cell vectors (a, b, c) equals at least (35, 35, 35) when using PBE functional or (22, 22, 22) when using HSE06 [30]. The crystal structures of α-$MoO_3$ and β-$MoO_3$ are taken from available crystallographic information files [31,32]. An optimization of the atomic positions of bulk structures was followed by a standard cell optimization (without spin polarization) as implemented in VASP using the screened hybrid functional HSE06 [30]. In case of α-$MoO_3$, the unit cell expanded in 010 directions, with only very small variations in the cell vectors *a* and *c*. For β-$MoO_3$, the cell parameters underwent only minor changes upon optimization [33]. The transition between α-$MoO_3$ and β-$MoO_3$ is calculated at different temperatures with inclusion of vibrational contributions using $2 \times 1 \times 2$ (α-$MoO_3$) and $1 \times 2 \times 1$ (β-$MoO_3$) supercells. The PBE + U approach with U = 6.3 eV (on site Coulomb) and J = 1 eV (on site exchange) was used, these values are in alignment with values used in earlier studies [34,35]. To obtain the work-functions and valence band positions (with respect to the vacuum) of both polymorphs, periodic slab models are constructed using experimental lattice constants of α-$MoO_3$-slab and vacuum of 20 Å in the y-direction. An α-$MoO_3$(010) surface slab of four van der Waals bonded α-sheets is taken and subsequently, the β-$MoO_3$-slab is constructed manually from the α-$MoO_3$-slab using ASE, maintaining the experimentally based lattice constants of the α-$MoO_3$-slab [36]. The work functions are calculated using spin polarization using PBE.

### *Thin film preparation*

Nanocrystalline thin films of $MoO_3$ were deposited onto indium-doped tin oxide ($SnO_2$: In, ITO; Resistivity 10–15 Ohm-cm) and onto n-type Si (100) wafer by reactive rf-magnetron sputtering (Advanced Process Technology Instruments, India). A molybdenum target (99.99% purity) was used and the process gas was a mixture of argon and oxygen (10–100% oxygen in argon). All the substrates were properly cleaned by

Please cite this article in press as: Kodan N, et al., Favourable band edge alignment and increased visible light absorption in β-$MoO_3$/α-$MoO_3$ oxide heterojunction for enhanced photoelectrochemical performance, International Journal of Hydrogen Energy (2018), https://doi.org/10.1016/j.ijhydene.2018.06.138